

High-shear treatment of single-walled carbon nanotube–superacid solutions as a pre-processing technique for the assembly of fibres and films

R D Booker¹, M J Green^{1,2}, H Fan¹, A N G Parra-Vasquez^{1,2}, N Behabtu^{1,2}, C C Young¹, R H Hauge^{1,3}, H K Schmidt¹, R E Smalley^{1,3†}, W-F Hwang¹, and M Pasquali^{1,2,3*}

¹Smalley Institute for Nanoscale Science and Technology, Rice University, Houston, Texas, USA

²Department of Chemical and Biomolecular Engineering, Rice University, Houston, Texas, USA

³Department of Chemistry, Rice University, Houston, Texas, USA

The manuscript was received on 16 February 2009 and was accepted after revision for publication on 9 June 2009.

DOI: 10.1243/17403499JNN123

Abstract: Single-walled carbon nanotubes (SWNTs) show great promise for use in a wide range of applications. One of the most promising avenues for attaining these applications is the dispersion of SWNTs at high concentrations in superacids, and their processing into macroscopic articles such as fibres or films. Fibres spun from SWNT/superacid dispersions indicate that the morphology of the starting SWNT material is reflected in the final morphology of the as-spun fibre. Here, we describe a method (termed disentanglement) of dispersing SWNTs in superacids and treating them using a high-shear, rotor/stator homogenizer, followed by coagulation to recover the solid SWNT material for use in fibre spinning. Several lines of experimental evidence (rheology and optical microscopy of the SWNTs in solution, scanning electron microscopy (SEM) of the coagulated material, and SEM of fibres spun from the coagulated material) show that this treatment radically improves the degree of alignment in the SWNTs' morphology, which in turn improves the dispersibility and processability. Raman microscopy and thermogravimetric analysis (TGA) before and after homogenization show that the treatment does not damage the SWNTs. Although this technique is particularly useful as a pre-processing step for fibre spinning of neat SWNT fibres, it is also useful for neat SWNT films, SWNT/polymer composites, and surfactant- or polymer-stabilized SWNT dispersions.

Keywords: single-walled carbon nanotube, single-walled carbon nanotubes, fibres, superacid, dispersion

1 INTRODUCTION

Individual single-walled carbon nanotubes (SWNTs) possess remarkable properties, with a Young's modulus of 1000 GPa [1], tensile strength above 30 GPa [2, 3], electrical conductivity better than copper (in the case of armchair SWNTs) [4–6], and thermal conductivity comparable to that of diamond [7, 8]. Potential SWNT applications span a wide range, from transistors [9] to chemical sensors [10] and, notably,

mechanical reinforcement as neat materials [11–13] or polymer composites [14–16]. The properties of individual nanotubes have not yet been fully realized in neat SWNT materials as well as polymer-SWNT composites, primarily owing to inadequate control of the SWNT structure in terms of alignment and packing (for neat materials) or dispersion (for composites), which in turn affect stress transfer in the material [13]. To fully exploit SWNTs' microscopic properties in neat macroscopic articles, the SWNTs must be processed into a dense, aligned state with good contact between SWNTs; in composites, the SWNTs must be dispersed individually (or nearly so). Here, we describe a pre-processing treatment, termed disentanglement, that facilitates subsequent dispersion of SWNTs into fluid phases. This

*Corresponding author: Department of Chemical and Biomolecular Engineering, Rice University, 6100 Main Street, MS-362, Houston, TX 77054, USA.

email: mp@rice.edu

†In memoriam, 28 October 2005.

processing step yields improved and more consistent alignment in acid-spun neat SWNT fibres. The disentanglement process is useful for pre-treating SWNTs for any process involving dispersion in acids (such as dispersion in polymer composites). Disentanglement is also a critical step in the formation of uniformly cut 'ultra-short' SWNTs for dispersion in polymer composites [17] and may be useful for SWNT films [18], dispersion in surfactants [19], or even dispersion via polymer wrapping [20–22].

Due to their high aspect ratio and the strong van der Waals attractions between them, individual SWNTs tend to aggregate into dense, robust, entangled networks of ropes [23], usually 10–20 nm in diameter and several microns in length, limiting their solubility and alignment. As such, SWNTs cannot be easily dispersed without some kind of chemical or physical surface modification to prevent this aggregation. Surfactants have been used to help separate and disperse individual SWNTs [24], but their use requires sonication and centrifugation at highly dilute concentrations (below 100 mg/L); moreover, fully removing surfactants from the final solid SWNT material is difficult. Superacids such as fuming sulphuric acid and chlorosulphonic acid have been used to disperse SWNTs at high concentrations (over 10 wt%). This technique is successful because the SWNTs become protonated and form charge-transfer complexes of individual nanotubes surrounded by sulphuric acid [25]. At low concentration, SWNT–acid mixtures are biphasic mixtures of a dilute isotropic phase of well-dispersed SWNTs in equilibrium with liquid crystalline domains with spaghetti-like mor-

phology [26, 27]. At sufficiently high SWNT concentration, these mixtures are liquid crystalline [27] and can be spun into continuous fibres [13, 28, 29] and cast into films [30].

SWNTs are wet spun by homogeneously mixing a high concentration of SWNT into a strong acid, extruding this viscous mixture (termed 'dope') through a needle-like orifice into a non-solvent (or 'coagulant') where the solvent is removed and the SWNT dope solidifies into a fibre. A similar technique is used to process rod-like polymers such as poly (p-phenylene terephthalamide) PPTA in sulphuric acid into Kevlar fibres [31]. Ericson *et al.* [13] mixed 8 wt% SWNTs in 102 per cent sulphuric acid (2 wt% excess SO₃), extruded the SWNT/acid dope through a needle (125–250 μm diameter), and coagulated the dope in water to arrive at a solid neat SWNT fibre. That article and related work [32] reported that the morphology of the starting SWNT material affects the morphology of the as-spun fibre (Fig. 1). Specifically, if the starting SWNT ropes are highly entangled prior to mixing in acid and spinning, the spun fibres typically do not attain a well-aligned, packed morphology. SWNTs packed into entangled ropes have little mobility, and this hinders their mixing into superacids – possibly yielding a non-equilibrium entangled gel of swollen SWNT ropes rather than a liquid crystal. This structure can hamper reorientation and alignment during fibre spinning. Here we present a scalable disentanglement process that promotes alignment of the SWNTs at the microscale and improves the properties of the resulting macroscopic fibre.

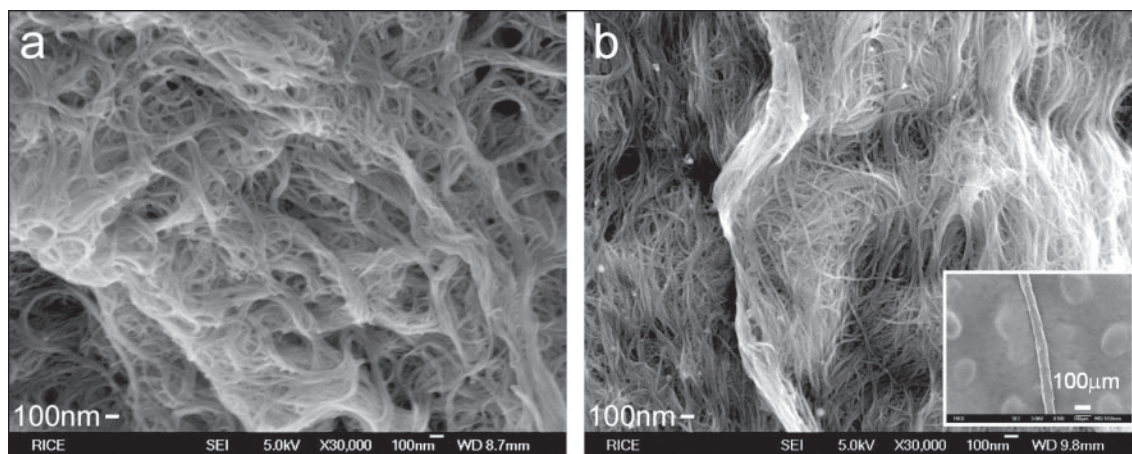


Fig. 1 Scanning electron microscopy (SEM) images of (a) purified HiPco SWNT and (b) the fibre that was wet-spun from the purified material using the method of reference [13]. The spinning utilized SWNTs from purified HiPco batch 120.2 at 10 wt% on 21 April 2004. The fibre reported in Fig. 2(b) of reference [13] showed very good alignment of individual SWNTs; this morphology was reproducible but was not typical. Most fibres produced directly from purified SWNT have less ordered morphology (b), depending on HiPco batch type and preprocessing methods. The scale bar at the bottom images (a) and (b) is 100 nm, and the inset scale bar is 100 μm

2 EXPERIMENTAL SECTION

SWNTs were produced by the HiPco process [33] and purified by multistep gas-phase oxidation in the presence of SF₆. The material was then washed in 6M HCl to remove catalyst and non-SWNT carbon [34]. This purification method essentially removes all non-SWNT carbon and lowers the metal content of the sample to less than 3 wt%. The purified SWNTs were dispersed at 0.25 wt% in 520 mL of 120 per cent H₂SO₄ (Alfa Aesar, 20 per cent SO₃, density 1.925 g/mL) in a tri-neck round bottom flask and homogenized at high speed (3500 r/min) with a rotor/stator immersion blender for 72 h. To prevent possible shear-induced heating of the SWNTs and potential high-temperature reactions with the acid, the entire mixing apparatus was wrapped with a cooling system that kept the solution at room temperature or below. The system was sealed to prevent SO₃ from escaping, with the exception of one flask port connected to a bubbler to release any pressure build-up. After 72 h of homogenization, the SWNTs were precipitated by coagulating the SWNT/acid solution into ice in a 4L Erlenmeyer flask. This aqueous acidic mixture was thoroughly washed with deionized water and vacuum filtered onto a 5 μm Millipore Durapore[®] membrane until neutral, to remove residual acid. Care was taken to remove all residual acid in the system to prevent potential SWNT oxidation during the subsequent high-temperature vacuum drying. After the filtration, the neutralized SWNTs were immersed in methanol and then diethyl ether in order to remove any residual water from the material; this water-removal step is critical for successful mixing and fibre spinning, since residual water could compromise SWNT protonation and dispersion. The SWNTs were then removed from the filtration apparatus and further dried in a vacuum oven at 85 °C.

During homogenization, samples were taken at progressive time increments (i.e. 5 min, 1 h, 3 h, etc.) up to 72 h, and rheological measurements, optical microscopy, and scanning electron microscopy (SEM) were performed to characterize each sample. Rheological characterization was performed on an ARES (TA Instruments) strain-controlled rotational rheometer [27]. Parallel plate fixtures (50 mm diameter) made of Hastelloy C were used to prevent corrosion. An anhydrous environment was maintained by blanketing the sample with a continuous flow of argon in addition to covering the sample surface with an inert, low-viscosity fluid, 25 mPa-s silicon oil. Optical microscopy was performed on a Zeiss Axioplan optical microscope. The SEM samples were water coagulated, neutralized, and placed in a vacuum oven at 85 °C. SEM measurements were performed on a JEOL 6500F thermal field emission electron microscope.

3 RESULTS AND DISCUSSION

Figure 2 shows the effects of the disentanglement process. As-produced (raw) HiPco SWNTs consist of entangled networks (Fig. 2(a)) of fine, randomly oriented ‘primordial’ ropes 10–20 nm in diameter. This randomly entangled network persists in the purified SWNTs (Fig. 2(b)) but in a more compact morphology. After disentanglement and coagulation, the SWNTs are locally aligned in ‘super ropes’ of 50 nm or more in diameter (Fig. 2(c)).

After disentanglement, the SWNTs are readily dispersed into fuming sulphuric acid without the aid of sonication. Figure 3 shows a side-by-side comparison of experiments where raw, purified, and disentangled SWNT powders are dusted into 120% sulfuric acid with minimal mixing in an anhydrous atmosphere. After 18 h, the raw and purified SWNTs aggregate,

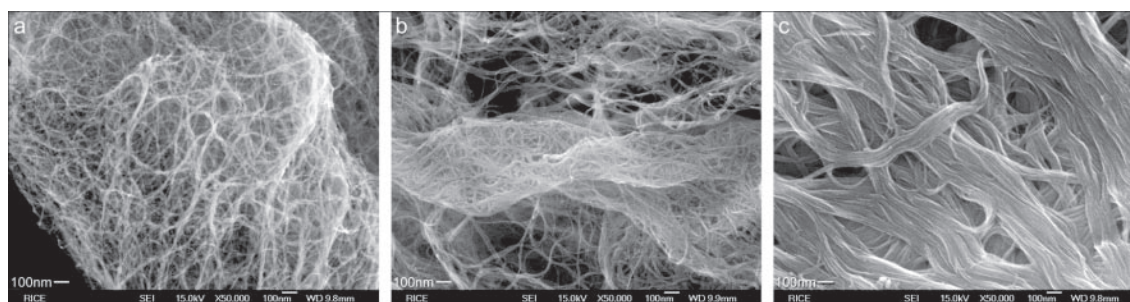


Fig. 2 SEM images of HiPco batch 188.3 showing the evolution of raw SWNTs into disentangled SWNTs. (a) Entangled network of raw HiPco SWNTs. (b) Tightly entangled network of purified HiPco SWNTs. (c) Aligned super ropes of 50 nm or more in diameter after 72 h of the rotor stator disentanglement process and subsequent coagulation. The scale bar at the bottom of each image is 100 nm

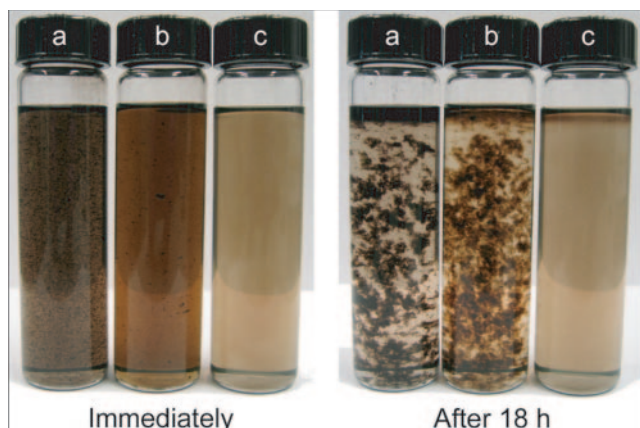


Fig. 3 Two photographs of 70 ppm of (a) raw, (b) purified, and (c) disentangled HiPco SWNTs immediately after immersion in 120 per cent sulphuric acid (left) and the same vials after 18 h (right). Both the raw and purified SWNTs aggregate whereas the disentangled SWNTs show uniform dispersion

whereas the disentangled does not. The presence of iron catalyst particles and fullerenes in the raw sample explains the difference in colour between raw and purified. Although the disentangled sample appears lighter in colour, it contains the same amount of SWNTs as the other samples.

The effects of the rotor/stator disentanglement process are compared to a control mixing method where the SWNTs are dispersed at the same concentration and simply stirred with a stir bar rather than being homogenized by the rotor/stator. The difference in morphology between samples disentangled by these two methods is shown in Fig. 4, which shows SEM images of the coagulated solution. Purified SWNTs are dispersed in 120 per cent H_2SO_4 and homogenized at high speed with a rotor/stator immersion blender for 5 min (Fig. 4(a)), an hour (Fig. 4(b)), and 24 h (Fig. 4(c)). After 5 min (Fig. 4(a)), the SWNT

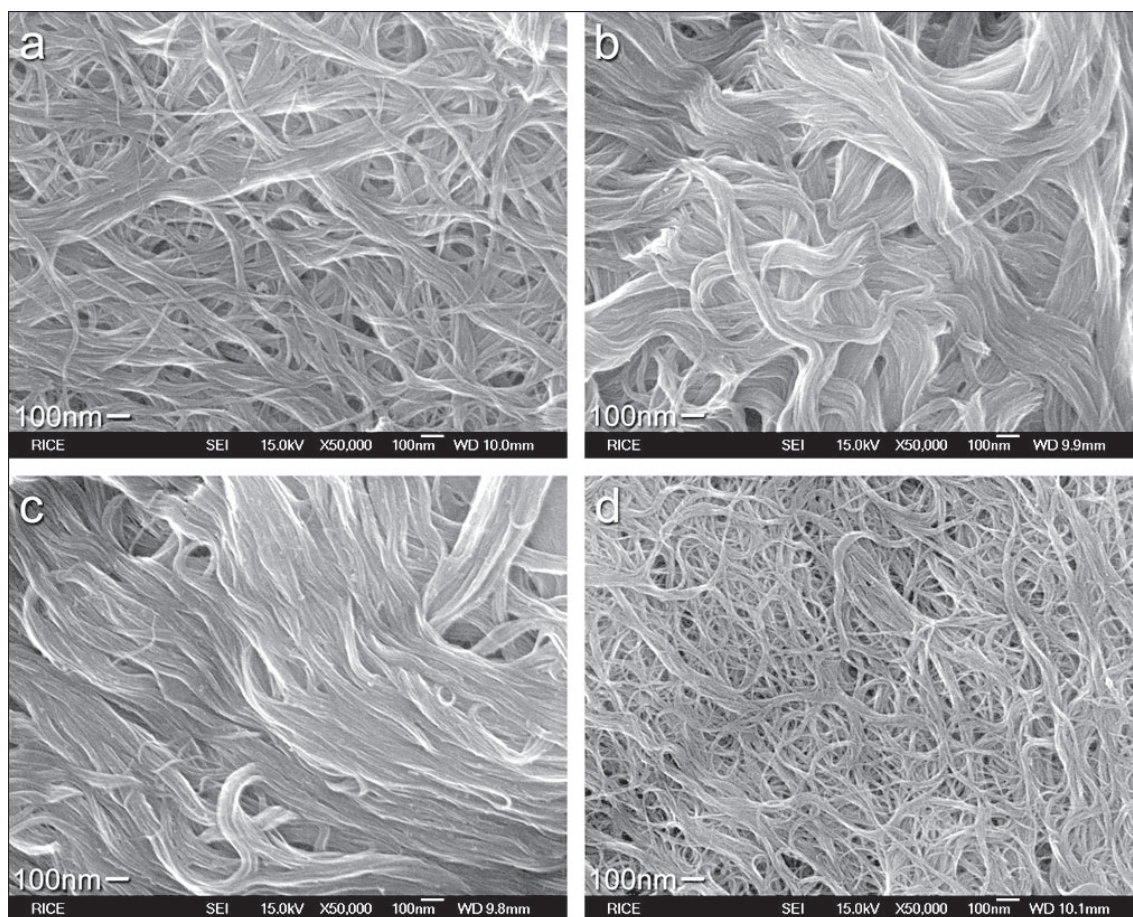


Fig. 4 SEM images of coagulated solution samples showing the dramatic change in morphology during disentanglement using the high-speed rotor/stator between (a) the first 5 min and (b) 1 h later. Within the first few minutes of disentanglement, larger rope structures are forming but are still entangled. After an hour, the SWNTs form larger, less entangled, continuous ropes. (c) After 24 h, these large rope structures show local alignment. (d) For comparison, instead of the rotor stator, the present authors performed the same experiment with mixing via stir bar for 24 h. The simple stir-bar method does not adequately break up the tightly entangled SWNT aggregates, nor create larger ropes, whereas the rotor/stator method does. The scale bar at the bottom of each image is 100 nm

morphology resembles the morphology of purified SWNT presented in Fig. 2(b), but the SWNTs are beginning to form larger ‘super ropes’. After 1 h, disentangled super ropes dominate and start to form aligned regions. After 24 h, the images show large regions of aligned ropes. This is in stark contrast to the simple stir-bar method which results in a morphology (Fig. 4(d)) that still resembles purified SWNT (Fig. 2(b)) even after 24 h of stirring.

Optical microscopy of the two samples (stir-bar method versus rotor/stator method) after 24 h is compared in Fig. 5. The stir-bar method (Fig. 5(a)) leaves undispersed material and large aggregates (up to 5 μm) whereas the rotor/stator breaks up all aggregates and helps to align and coalesce the SWNT domains (Fig. 5(b)). Birefringence of the rotor/stator sample (Fig. 5(d)) clearly illustrates large regions of aligned domains as compared to the stir-bar method (Fig. 5(c)), which shows very little alignment.

Rheological measurements confirm a rapid drop in viscosity of the SWNT/acid dispersion associated with the rotor/stator method as compared to that associated with the stir-bar method. After 12 h, the rotor/stator-mixed sample reached a steady state whereas the viscosity of the stir-bar-mixed sample was four times that of the rotor/stator-mixed sample (Fig. 6) and remained so even after ten days. The inset of Fig. 6 illustrates the shear rate in relation to viscosity for the 12 h sample. This representative sample illustrates SWNT shear thinning, a result of the individual SWNT’s high aspect ratio and their arrangement into thread-like, aligned, liquid-crystalline domains (dubbed ‘spaghetti’ [27]).

Figure 7 depicts SEM of fibres spun from the stir-bar sample and rotor/stator sample. Again, the morphology of the fibre spun from the disentangled SWNT material shows a substructure composed of much larger SWNT ropes.

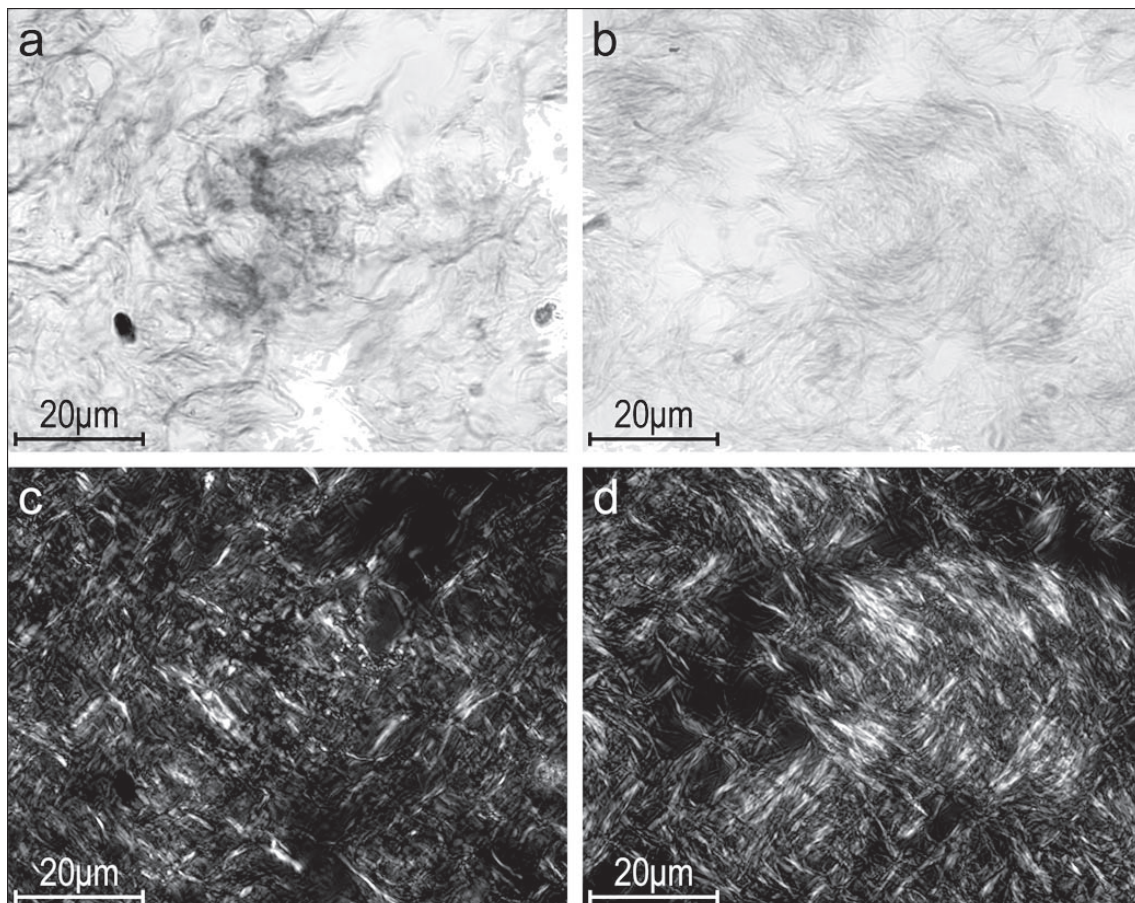


Fig. 5 Optical microscopy images of HiPco batch 188.3 after 24 h of disentanglement using (a) a stir bar and (b) a high-speed rotor/stator. The sample homogenized by the stir bar appears dispersed but is still entangled, containing visible aggregates and undispersed material. The sample homogenized by the rotor/stator contains aligned thread-like liquid-crystalline ‘spaghetti’ domains and no aggregates. Images (c) and (d) are images under cross polars of (a) and (b) respectively. The scale bar at the bottom of each image is 20 μm

Raman spectra are obtained on a Renishaw RamaScope with 785 nm diode laser for the raw, purified, and disentangled SWNTs and are shown in Fig. 8. The results show that these are undoubtedly

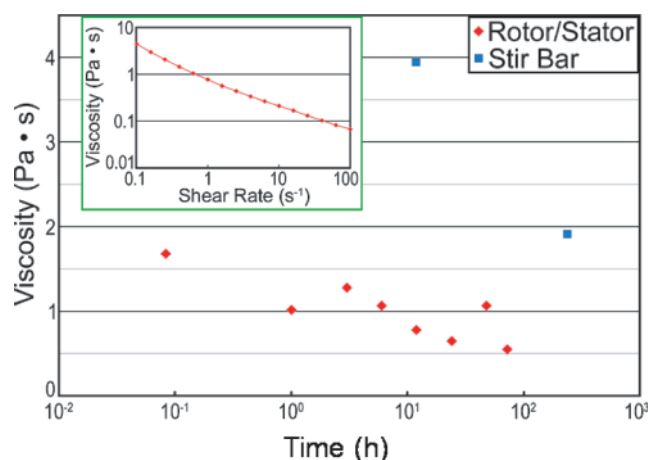


Fig. 6 Rheological data (viscosity at a shear rate of 1/s as a function of total disentangling time) comparing the two disentangling methods (rotor/stator versus stir bar). The viscosity of the solution homogenized by the rotor/stator method (red) quickly decreases and reaches a steady state after 12 h. The inset illustrates shear thinning of the 12 h sample. Because of their high aspect ratio, SWNTs exhibit shear thinning at all measured shear rates. The viscosity of the solution homogenized by the stir-bar method (blue) is four times higher, decreases at a much slower rate, and never achieves the same low viscosity as that of the sample homogenized by the rotor/stator method. The inset shows the shear-thinning behaviour of the solution homogenized by the rotor/stator method, and this is consistent with the formation of liquid-crystalline domains which align with increasing shear rate

pristine single-walled carbon nanotubes with the SWNT-unique radial breathing mode (RBM at 100–300 cm^{-1}), the disorder mode (D-band at around 1300 cm^{-1}), and the characteristic tangential mode (G-band at 1590 cm^{-1}). For all the samples, the intensity ratio (D/G ratio) was less than 1/20, indicating that the SWNT sidewalls were pristine. This suggests that the disentangled SWNTs were neither damaged nor functionalized during the high-shear disentangling process. (The G-band shifts in the presence of acid; this process is reversible if the acid is removed because the acid imparts a delocalized positive charge rather than covalent functionalization.) Thermogravimetric analysis (TGA) also shows

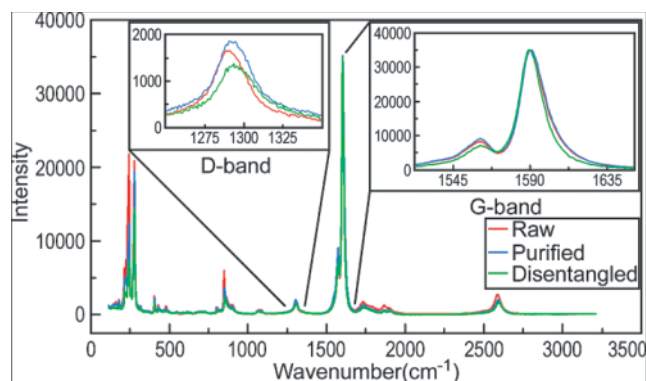


Fig. 8 Raman spectra (785 nm laser) of raw, purified, and disentangled HiPco batch 188.3 showing that the use of fuming sulphuric acid does not functionalize the nanotubes. Spectra are normalized to the graphite band (G-band at 1590 cm^{-1}). If the SWNTs were functionalized, the defect band (D-band at 1300 cm^{-1}) would increase relative to the graphite band. The D/G ratios are less than 1/20, indicating that the SWNT sidewalls are pristine (raw 0.028; purified 0.038; and disentangled 0.024)

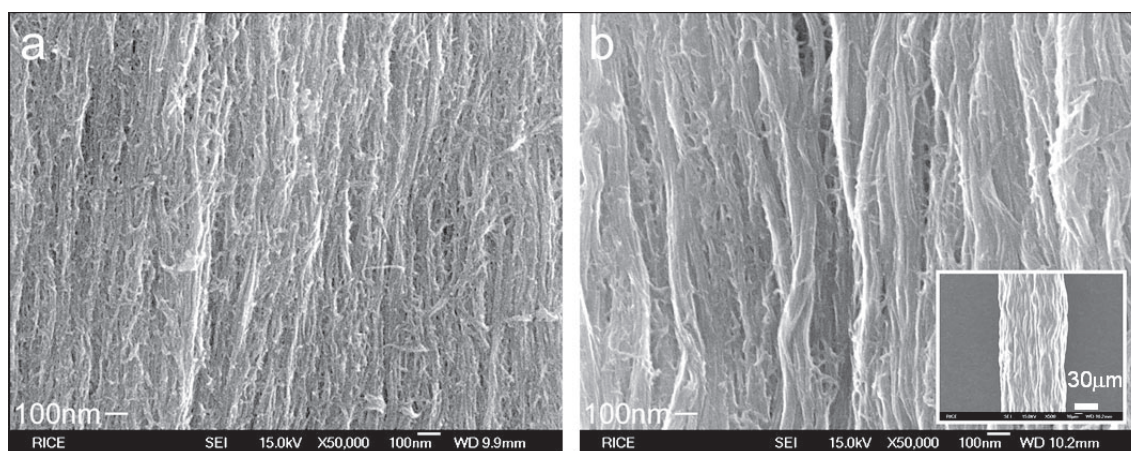


Fig. 7 SEM images of HiPco batch 188.3 after spinning into a fibre [13] using SWNT from the (a) stir-bar-mixed sample and (b) rotor/stator-mixed sample. Alignment measurements from Raman spectroscopy show a ratio of 5:1 for the stir bar and 13:1 for the rotor/stator. The scale bar at the bottom images (a) and (b) is 100 nm, and the inset scale bar is 30 μm

typical weight loss associated with purified and disentangled nanotubes. There were negligible amounts of water (100 °C) and sulphuric acid (290 °C) as indicated by no significant weight loss at the temperatures associated with these compounds. As stated before, the presence of water hinders protonation of the SWNT and successful fibre spinning, so the elimination of water is critical.

The mechanism of the disentanglement process works as follows. As the rotor spins (Fig. 9), it draws the SWNTs axially into the dispersion head and creates radial flow through the slots of the rotor/stator arrangement. It is this extensional force, along with the cross forces in the shear gap, that progressively eliminate SWNT entanglements and promote the alignment and coalescence of SWNT domains into larger, aligned structures. This occurs for the following reasons: when SWNT material is placed in fuming sulphuric acid, the acid rapidly diffuses into the rope-like structures, intercalates between the SWNTs, and creates threadlike ‘spaghetti’ liquid-crystalline domains [27]; this rapid diffusion process has previously been observed in fibre-swelling experiments [13]. The motion of the nanotubes is mainly restricted to the lengthwise direction of these domains. In the case of purified SWNT samples dispersed in fuming sulphuric acid, these domains are highly restricted in their relative motion owing to the entanglements, so there is little chance for the domains to disentangle, disperse, align, or coalesce. Thus, little to no change in morphology is observed (as in Fig. 4(d)). In the case of SWNT samples that are disentangled using the rotor/stator set-up, the kinetics of the liquid–crystalline domains are no longer hindered because the strong viscous forces pull on the spaghetti domains, facilitating the break-up of entanglement points. This not only aids in dispersion, but it also allows the liquid–crystalline domains to reorient, flow-align, and coalesce. When this disentangled sample is coagulated, the morphology shows super ropes that are much larger in diameter than the ropes observed in the starting

material, as shown in Fig. 4. Also, in the purified SWNT material dispersed without disentanglement, optical microscopy shows the presence of densely packed SWNT aggregates; the viscous forces of the disentanglement process breaks these aggregates apart and allows acid to intercalate and disperse the SWNTs. These aggregates are caused by the purification process and can lead to major problems in fibre spinning, so their elimination is essential.

4 CONCLUSIONS

We have developed a treatment method for SWNT material in which the SWNTs are dispersed in superacid and homogenized using a high-shear rotor/stator. Our results show significant changes in the sample morphology without damage to the SWNTs. The high-shear forces align the SWNT liquid crystalline domains in the local direction of flow, allowing for domain coalescence. When coalesced and quenched, the solid SWNT morphology consists of large SWNT ropes; this morphology is reflected in better order and coalescence in fibres spun from the homogenized material. This change in morphology is beneficial for SWNT fibres because improved alignment and improved frictional contact between the constituent SWNTs improve the mechanical properties of the fibre. This technique can also be used to pre-treat SWNTs for processing of SWNT/superacid dopes into aligned films and to aid in the production of ultra-short SWNTs [17]. It may also prove useful for the production of surfactant- or polymer-stabilized SWNT dispersions and SWNT/polymer composites.

ACKNOWLEDGEMENTS

The authors acknowledge the help of Steve Ripley, Carter Kittrell, Jonathan Allison, Virginia Davis, Haiqing Peng, Zheyi Chen, and Wade Adams. Funding was provided by the Office of Naval Research under Grant N00014-01-1-0789, AFOSR grant FA9550-06-1-0207, AFRL agreements FA8650-07-2-5061 and 07-S568-0042-01-C1, the Robert A. Welch Foundation grant C-1668, and the Evans-Attwell Welch Postdoctoral Fellowship.

© Authors 2009

REFERENCES

- 1 Krishnan, A., Dujardin, E., Ebbesen, T. W., Yianilos, P. N., and Treacy, M. M. J. Young's modulus of single-walled nanotubes. *Phys. Rev. B*, 1998. **58**(20), 14 013–14 019.

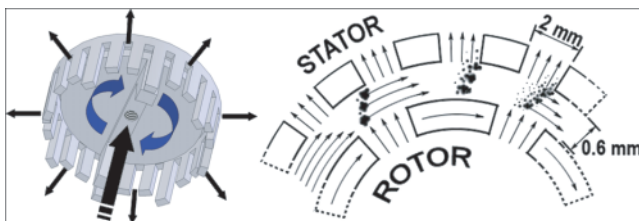


Fig. 9 The high-speed rotation of the rotor automatically draws the SWNTs axially into the dispersion head, forcing them radially through the slots of the rotor/stator arrangement. The flow in the small gap between the rotor and the stator produces strong shearing forces that promote dispersion and alignment of the SWNTs

- 2 Walters, D. A., Ericson, L. M., Casavant, M. J., Liu, J., Colbert, D. T., Smith, K. A., and Smalley, R. E. Elastic strain of freely suspended single-wall carbon nanotube ropes. *Appl. Phys. Lett.*, 1999, **74**(25), 3803–3805.
- 3 Yu, M. F., Files, B. S., Arepalli, S., and Ruoff, R. S. Tensile loading of ropes of single wall carbon nanotubes and their mechanical properties. *Phys. Rev. Lett.*, 2000, **84**(24), 5552–5555.
- 4 Thess, A., Lee, R., Nikolaev, P., Dai, H., Petit, P., Robert, J., Xu, C., Lee, Y. H., Kim, S. G., Rinzler, A. G., Colbert, D. T., Scuseria, G. E., Tománek, D., Fischer, J. E., and Smalley, R. E. Crystalline ropes of metallic carbon nanotubes. *Sci.*, 1996, **273**(5274), 483–487.
- 5 Tans, S. J., Devoret, M. H., Dai, H., Thess, A., Smalley, R. E., Geerligs, L. J., and Dekker, C. Individual single-wall carbon nanotubes as quantum wires. *Nature*, 1997, **386**(6624), 474–477.
- 6 McEuen, P. L., Fuhrer, M. S., and Park, H. K. Single-walled carbon nanotube electronics. *IEEE Trans. Nanotechnol.*, 2002, **1**(1), 78–85.
- 7 Hone, J., Whitney, M., Piskoti, C., and Zettle, A. Thermal conductivity of single-walled carbon nanotubes. *Phys. Rev. B*, 1999, **59**(4), R2514–R2516.
- 8 Che, J. W., Cagin, T., and Goddard, W. A. Thermal conductivity of carbon nanotubes. *Nanotechnol.*, 2000, **11**(2), 65–69.
- 9 Seidel, R., Graham, A. P., Unger, E., Duesberg, G. S., Liebau, M., Steinhögl, W., Kreupl, F., Hoenlein, W., and Pompe, W. High-current nanotube transistors. *Nano Lett.*, 2004, **4**(5), 831–834.
- 10 Besteman, K., Lee, J.-O., Wiertz, F. G. M., Heering, H. A., and Dekker, C. Enzyme-coated carbon nanotubes as single-molecule biosensors. *Nano Lett.*, 2003, **3**(6), 727–730.
- 11 Vigolo, B., Pénicaud, A., Coulon, C., Sauder, C., Paillet, R., Journet, C., Bernier, P., and Poulin, P. Macroscopic fibers and ribbons of oriented carbon nanotubes. *Sci.*, 2000, **290**(5495), 1331–1334.
- 12 Dalton, A. B., Collins, S., Munoz, E., Razal, J. M., Ebron, V. H., Ferraris, J. P., Coleman, J. N., Kim, B. G., and Baughman, R. H. Super-tough carbon-nanotube fibres – These extraordinary composite fibres can be woven into electronic textiles. *Nature*, 2003, **423**(6941), 703–703.
- 13 Ericson, L. M., Fan, H., Peng, H., Davis, V. A., Zhou, W., Sulpizio, J., Wang, Y., Booker, R., Vavro, J., Guthy, C., Parra-Vasquez, A. N. G., Kim, M. J., Ramesh, S., Saini, R. K., Kittrell, C., Lavin, G., Schmidt, H., Adams, W. W., Billups, W. E., Pasquali, M., Hwang, W.-F., Hauge, R. H., Fischer, J. E., and Smalley, R. E. Macroscopic, neat, single-walled carbon nanotube fibers. *Science*, 2004, **305**(5689), 1447–1450.
- 14 Moniruzzaman, M. and Winey, K. I. Polymer nanocomposites containing carbon nanotubes. *Macromolecules*, 2006, **39**(16), 5194–5205.
- 15 Kumar, S., Dang, T. D., Arnold, F. E., Bhattacharyya, A. R., Min, B. G., Zhang, X., Vaia, R. A., Park, C., Adams, W. W., Hauge, R. H., Smalley, R. E., Ramesh, S., and Willis, P. A. Synthesis, structure, and properties of PBO/SWNT composites. *Macromolecules*, 2002, **35**(24), 9039–9043.
- 16 Kobashi, K., Zheyi, C., Lomeda, J., Rauwald, U., Hwang, W.-F., and Tour, J. M. Copolymer of single-walled carbon nanotubes and poly(p-phenylene benzobisoxazole). *Chem. Mater.*, 2007, **19**(2), 291–300.
- 17 Chen, Z. Y., Kobashi, K., Rauwald, U., Booker, R., Fan, H., Hwang, W. F., and Tour, J. M. Soluble ultra-short single-walled carbon nanotubes. *J. Am. Chem. Soc.*, 2006, **128**(32), 10568–10571.
- 18 Wu, Z. C., Chen, Z., Du, X., Logan, J. M., Sippel, J., Nikolou, M., Kamaras, K., Reynolds, J. R., Tanner, D. B., Hebard, A. F., and Rinzler, A. G. Transparent, conductive carbon nanotube films. *Sci.*, 2004, **305**(5688), 1273–1276.
- 19 Huang, L. M., Cui, X., Dukovic, G., and O'Brien, S. P. Self-organizing high-density single-walled carbon nanotube arrays from surfactant suspensions. *Nanotechnol.*, 2004, **15**(11), 1450–1454.
- 20 O'Connell, M. J., Boul, P., Ericson, L. M., Huffman, C., Wang, Y., Haroz, E., Kuper, C., Tour, J., Ausman, K. D., and Smalley, R. E. Reversible water-solubilization of single-walled carbon nanotubes by polymer wrapping. *Chem. Phys. Lett.*, 2001, **342**(3–4), 265–271.
- 21 Star, A. and Stoddart, J. F. Dispersion and solubilization of single-walled carbon nanotubes with a hyperbranched polymer. *Macromolecules*, 2002, **35**(19), 7516–7520.
- 22 Star, A., Stoddart, J. F., Steuerman, D. W., Diehl, M. R., Boukai, A., Wong, E. W., Yang, X., Chung, S. W., Choi, H., and Heath, J. R. Preparation and properties of polymer-wrapped single-walled carbon nanotubes. *Angewandte Chemie-Int. Edn*, 2001, **40**(9), 1721–1725.
- 23 Liu, J., Rinzler, A. G., Dai, H., Hafner, J. H., Kelley Bradley, R., Boul, P. J., Lu, A., Iverson, T., Shelimov, K., Huffman, C. B., Rodriguez-Macias, F., Shon, Y.-S., Lee, T. R., Colbert, D. T., and Smalley, R. E. Fullerene pipes. *Sci.*, 1998, **280**(5367), 1253–1256.
- 24 Islam, M. F., Rojas, E., Bergey, D. M., Johnson, A. T., and Yodh, A. G. High weight fraction surfactant solubilization of single-wall carbon nanotubes in water. *Nano Lett.*, 2003, **3**(2), 269–273.
- 25 Ramesh, S., Ericson, L. M., Davis, V. A., Saini, R. K., Kittrell, C., Pasquali, M., Billups, W. E., Adams, W. W., Hauge, R. H., and Smalley, R. E. Dissolution of pristine single walled carbon nanotubes in superacids by direct protonation. *J. Phys. Chem. B*, 2004, **108**(26), 8794–8798.
- 26 Rai, P. K., Pinnick, R. A., Parra-Vasquez, A. N. G., Davis, V. A., Schmidt, H. K., Hauge, R. H., Smalley, R. E., and Pasqu, M. Isotropic-nematic phase transition of single-walled carbon nanotubes in strong acids. *J. Am. Chem. Soc.*, 2006, **128**, 591–595.
- 27 Davis, V. A., Ericson, L. M., Parra-Vasquez, A. N. G., Fan, H., Wang, Y., Prieto, V., Longoria, J. A., Ramesh, S., Saini, R. K., Kittrell, C., Billups, W. E., Adams, W. W., Hauge, R. H., Smalley, R. E., and Pasquali, M. Phase Behavior and rheology of SWNTs in superacids. *Macromolecules*, 2004, **37**(1), 154–160.
- 28 Wang, Y., Ericson, L. M., Kittrell, C., Kim, M. J., Shan, H., Fan, H., Ripley, S., Ramesh, S., Hauge, R. H., Adams, W. W., Pasquali, M., and Smalley, R. E. Revealing the substructure of single-walled carbon nanotube fibers. *Chem. Mater.*, 2005, **17**(25), 6361–6368.

- 29 Behabtu, N., Green, M. J., and Pasquali, M.** Carbon nanotube-based neat fibers. *Nano Today*, 2008, **3**(5–6), 24–34.
- 30 Sreekumar, T. V., Liu, T., Kumar, S., Ericson, L. M., Hauge, R. H., and Smalley, R. E.** Single-wall carbon nanotube films. *Chem. Mater.*, 2003, **15**(1), 175–178.
- 31 Jiang, H., Adams, W. W., and Eby, R. K.** High performance polymer fibers. In *Materials Science and Technology: Structure and Properties of Polymers*, Vol. 12 (Eds R. W. Cahn, P. Haasen, and E. J. Kramer), 1993 (Wiley-VCH).
- 32 Ericson, L. M.** Macroscopic neat single-wall carbon nanotube fibers. In *Physics and Astronomy*, 2003 (Rice University, Houston, Texas).
- 33 Bronikowski, M. J., Willis, P. A., Colbert, D. T., Smith, K. A., and Smalley, R. E.** Gas-phase production of carbon single-walled nanotubes from carbon monoxide via the HiPco process: A parametric study. *J. Vacuum Sci. Technol., A – Vacuum Surf. Films*, 2001, **19**(4), 1800–1805.
- 34 Xu, Y. Q., Peng, H. Q., Hauge, R. H., and Smalley, R. E.** Controlled multistep purification of single-walled carbon nanotubes. *Nano Lett.*, 2005, **5**(1), 163–168.